ELSEVIER International Journal of Mass Spectrometry and Ion Processes 142 (1995) 143–150

International Journal of Mass Spectrometry and Ion Processes

Enhanced accumulated trapping efficiency using an auxiliary trapping electrode in an external source Fourier transform ion cyclotron resonance mass spectrometer

Steven A. Hofstadler, Qinyuan Wu, James E. Bruce, Ruidan Chen, Richard D. Smith*

Chemical Sciences Department and Environmental Molecular Sciences Laboratory, Pacific Northwest Laboratory, Richland, WA 99352, USA

Received 22 February 1994; accepted 2 December 1994

Abstract

A scheme for the enhanced accumulation of ions injected into the trapped ion cell of a Fourier transform ion cyclotron resonance (FTICR) mass spectrometer from an external electrospray ionization source is described. This method utilizes an auxiliary electrode positioned outside the trapped ion cell which increases the effective collisional path length for ions traversing the trapped ion cell. A comparison made between pressure-assisted accumulated trapping in a symmetric trapping well, an asymmetric trapping well, and a symmetric trapping well with that for the addition of an auxiliary electrode indicates that trapping efficiency can be significantly improved when an auxiliary electrode trapping configuration is utilized.

Keywords: Accumulated trapping; Asymmetric ion accumulation; Auxiliary electrode; External source; Fourier transform ion cyclotron resonance; Ion trapping; Trapped ion cell

1. Introduction

Fourier transform ion cyclotron resonance (FTICR) mass spectrometry has seen rapid growth in recent years because of advances in both instrumentation and experimental methodology [1–5]. These advances cover many aspects of the technique, including improved external source interfaces [6–8], novel trapped ion manipulation techniques [9–12], and post-acquisition processing techniques to improve spectral quality [13,14]. The application of FTICR to b.che.cally related problems has seen explosive growth due primarily to the coupling of the technique with alternative ionization schemes such as matrix assisted laser desorption ionization (MALDI) [15], fast ion bombardment (FAB) [16], liquid secondary ionization mass spectrometry (LSIMS) [17] and electrospray ionization (ESI) [7,18,19]. Once the necessary pressure differentials are provided (ESI takes place at atmospheric pressure, whereas FTICR is best performed at $< 10^{-9}$ Torr), ESI is particularly amenable to FTICR

* Corresponding author.

SSDI 0168-1176(95)04141-9

detection, as the resulting multiply charged electrosprayed ions fall within an m/z range in which the mass accuracy and resolving power of FTICR are unparalleled. Mass spectra with low parts per million mass errors and resolution in excess of 10^6 have resulted from the ESI–FTICR combination [13,20].

The coupling of an atmospheric pressure technique to a high vacuum detection method such as FTICR is realized only through the use of multiple stages of differential pumping and an efficient means of transferring ions from the ionization source to the trapped ion cell. There are several methods typically used for the injection of ions into the trapped ion cell, including magnetic field focusing [8], electrostatic lens injection [21], and r.f. only quadrupole injection [6]. Injecting ions into the trapped ion cell is only part of the challenge; efficient utilization of the impinging ion beam is of paramount importance for the acquisition of mass spectra with high sensitivity. In this work, we will demonstrate variations of accumulated trapping which provide significant improvement in trapping efficiency and spectral resolution. As will be demonstrated, the improvements realized with these ion accumulation schemes are strongly tied to the kinetic energy distribution of the ion beam reaching the trapped ion cell. The addition of an auxiliary electrode behind the trapped ion cell is shown to result in the accumulation of a broader range of ion kinetic energies, resulting in improved ion accumulation efficiencies.

2. Experimental

The FTICR mass spectrometer used in these studies has been described in considerable detail elsewhere [19], so only a brief description is given here. Protein solutions containing 0.5–1.0 mg ml^{-1} of analyte in 5% HOAc are infused at a rate of 0.5 μl min^{-1} using a Harvard Apparatus (South Natick, MA) syringe pump. Ions are formed by electrospray ionization in a modified Analytica (Branford, CT) ESI source which has been equipped with a heated metal capillary to assist in ion desolvation. Ions are transported through the magnetic field gradient using two sets of r.f. only quadrupoles. After exiting the lens stack in the ESI source, the ion beam passes through a mechanical shutter assembly which separates the source region from the first section of the r.f. only quadrupole guide. The first section of the quadrupole guide is 15 cm long and terminates at a second shutter assembly which, when in the open position, constitutes a 3 mm conductance limit. The second section of the r.f. only quadrupole guide is 110 cm in length, and extends from the second shutter to the trapped ion cell, which is positioned in the center of a 7 T superconducting magnet. All aspects of pulse sequence timing, data acquisition and data manipulation are controlled by an IonSpec (Irvine, CA) Omega data system. The trapped ion cell used in these studies measures 5 cm × 5 cm × 7.6 cm in length and has holes in the front and rear trap plates measuring approximately 4 and 6 mm, respectively. The standard cell mounted filament assembly was removed for these studies and a planar gold electrode was mounted in its place. During the period of ion injection (typically 50–100 ms), the pressure in the trapped ion cell is raised to $\approx 10^{-4}$ Torr by introduction of dry nitrogen gas through a piezoelectric pulsed gas inlet to enhance ion accumulation and axialization. Pressure in the trapped ion cell returns to base level ($< 10^{-9}$ Torr) within a few seconds, at which time a swept frequency excite over the bandwidth of interest is applied to the excitation plates. The time domain signals are zero filled once and apodized with a full Hanning windowing function prior to Fourier transformation.

3. Results and discussion

3.1. Accumulated trapping

The initial ESI–FTICR experiments of Henry et al. [22] utilized a trapping technique referred to as gated trapping [23], in which the front trap plate is grounded during ion injection and rapidly reinstated to establish a trapping well such that a portion of the ion beam has insufficient kinetic energy to escape from the cell. Although this technique can be used in conjunction with continuous ionization sources, it is most efficient and ideally suited for pulsed ionization or injection conditions, such as with TOF–FTICR [24] or MALDI–FTICR [25]. Accumulated trapping [24] is more commonly employed with continuous ion sources. With this technique, the trapping potentials are adjusted to mimic the kinetic energy of the impinging ion beam [26]. Ions having sufficient z-axis kinetic energy to enter the trapped ion cell can be decelerated such that they have insufficient kinetic energy to escape the established potential well. The addition of a pulsed collision gas is typically used to enhance in-cell deceleration and thus increase accumulation efficiency. Hofstadler and Laude have demonstrated that accumulated trapping can, under the appropriate conditions, distinguish individual components in a protein mixture based on differences in ion kinetic energies [27]. Beu et al. have demonstrated that accumulated trapping is effective only for a narrow "slice" of kinetic energies [7]; at 3×10^{-6} Torr accumulated trapping is efficient only for a range of kinetic energies < 0.5 eV/q wide.

Studies by both Beu et al. [7] and Hofstadler and Laude [26,27] suggest that the efficiency of accumulated trapping can be increased by either narrowing the kinetic energy distribution of the ion beam or increasing the number of collisions (and thus the extent of ion deceleration) in the trapped ion cell. Although narrowing the kinetic energy distribution from the ESI source may be possible to some extent with higher order field correction electrodes, the ideal case of a monoenergetic ion beam seems unlikely, as additional phenomena such as charge transfer and velocity slip within the supersonic expansion [28] add to natural broadening of the kinetic energy distribution. To increase the number of collisions in the trapped ion cell, one could either increase the length of the cell (effectively increasing the path length over which an ion can suffer a collision in the cell) or increase the background pressure (thus increasing the collision frequency) in the cell. At present our system undergoes pressure excursions of up to $\approx 10^{-4}$ Torr during ion injection; significantly higher pressure does not appear to improve accumulation efficiency and may actually compromise spectral quality owing to an increased rate of growth of magnetron motion. The trapped ion cell used in these studies is 7.6 cm in length; we observed that with significantly longer cells the increased accumulation efficiency was more than offset by the degraded spectral quality, most likely due to the anharmonic electric fields and less homogeneous magnetic fields experienced by the ion ensemble.

3.2. Accumulation in an asymmetric potential well

An alternative accumulation configuration is realized by increasing the effective collisional path length which results from injecting ions into a potential well in which the back trap plate is biased at a higher potential than the front trap plate. Some ions which have sufficient kinetic energy to enter the trap are inadequately decelerated to be otherwise trapped. These ions are reflected by the higher potential on the rear trap plate and traverse the trapped ion cell in the other direction, nearly doubling the in-cell path length of the

ion beam. This concept is best illustrated by considering Figs. 1(a) and 1(b), which show the z-axis trapping potential of the trapped ion cell [29] when a symmetric and an asymmetric potential configuration is applied. Consider an ion with a kinetic energy of 5.8 eV/q entering the symmetric well in Fig. 1(a). If we assume that deceleration due to collisions over a 7.6 cm path length results in a loss of 0.2 eV/q , the ion will pass completely through the cell and will not be trapped. If that same ion now enters the well in Fig. 1(b), it will penetrate the cell until it encounters a potential equivalent to its initial kinetic energy minus the kinetic energy lost due to collisions, and will be reflected to again traverse the trapped ion cell traveling in the opposite direction. The overall ion trajectory constitutes a "round trip" through the trapped ion cell and, in this case, results in sufficient collisional deceleration to permit the trapping of the ion (i.e. in the asymmetric well the ion path length was increased from 7.6 cm to nearly 15 cm). Fig. 2 demonstrates the increased accumulation efficiency when the voltage on the rear trapping electrode is offset compared with the front trapping electrode voltage.

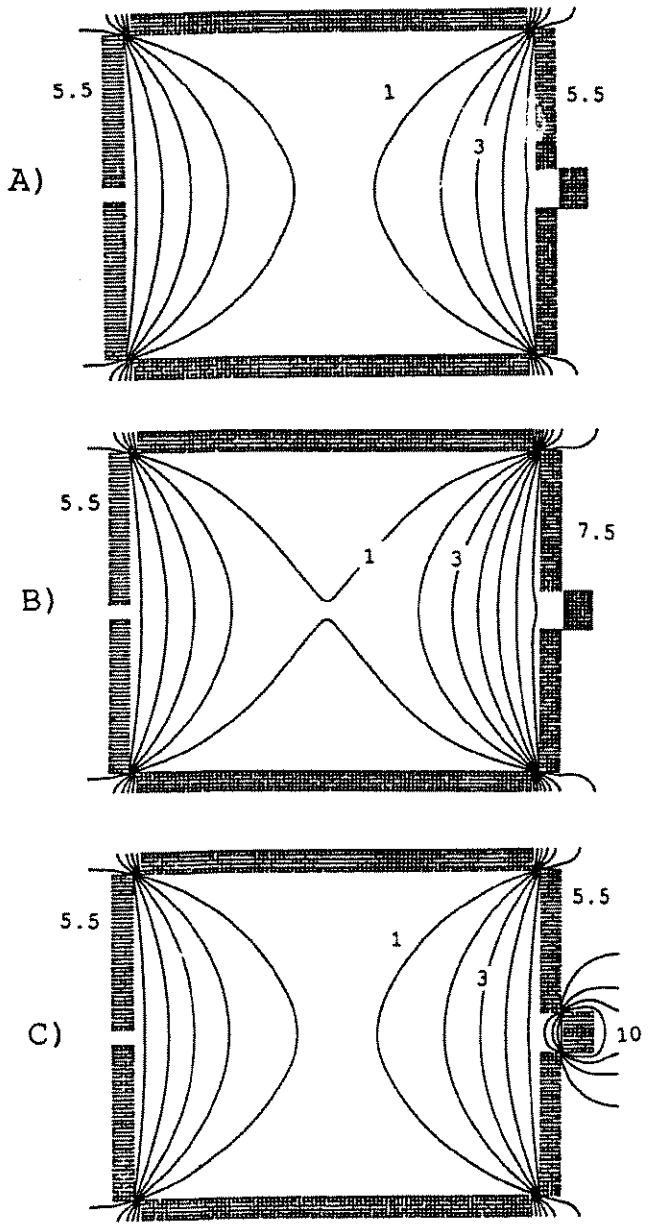

Fig. 1. SIMION simulation of the three trapping schemes: (a) both trap plates are at 5.5 V; (b) the front (left) plate is at 5.5 V and the back at 7.5 V; (c) as in (a), except that the auxiliary plate is at 10 V. The numbers indicate potentials of the contours in volts.

3.3. Accumulation with an auxiliary electrode

A potential shortfall of the asymmetric accumulation technique is that, if the asymmetry in the accumulation well is excessive, the effective path length will be substantially reduced compared with a symmetric well, as such a configuration allows significantly less penetration of the ion beam. For example, a potential well in which the front and rear trap

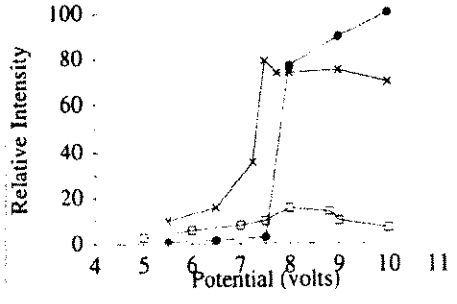

Fig. 2. Detected ion intensities using the three trapping schemes shown in Fig. 1. The x axis potentials refer to (□) both trap plates and the auxiliary electrode; (×) the back trap plate and auxiliary electrode with the front trap plate at 5.5 V; (●) the auxiliary electrode while both the front and back trap plates are at 5.5 V.

plates are maintained at 0.5 V and 100 V respectively during ion injection allows only slight penetration, and thus a short collisional path length, for low energy ions. As demonstrated in Fig. 1(b), even with a potential difference of 2 V (i.e. 5.5 V on the front and 7.5 V on the back), the potential well is notably shallower than in Fig. 1(a). A greater electrostatic potential on the rear trap plate serves to increase the path length for higher energy ions (i.e. ions having kinetic energies comparable to the potential applied to the rear trapping electrode), but lower energy ions may be reflected sooner and experience a shorter effective path length. To overcome this undesirable effect, and to maximize the effective path length for all ions regardless of kinetic energy, we have installed an auxiliary electrode behind the trapped ion cell as shown in Fig. 1(c). During ion injection the auxiliary electrode is raised to a potential which exceeds the kinetic energy of the ion beam. Ions which are too energetic to be collisionally decelerated and trapped during the first pass through the cell are reflected at the auxiliary electrode and are forced to re-enter the cell for additional deceleration and subsequent accumulation. The auxiliary electrode is positioned ≈ 1 mm from the rear trap plate as shown in Fig. 1(c).

By doubling the effective collisional path length of ions traversing the trapped ion cell, the kinetic energy range of ions subject to collisional accumulation is doubled. Thus, if an ion beam loses 0.5 eV/q of kinetic energy during one traversal of the trapped ion cell [7], it will lose 1.0 eV/q kinetic energy during a round-trip excursion through the trapped ion cell. The effect on accumulation efficiency of doubling the kinetic energy acceptance bandwidth is highly dependent on the width of the kinetic energy distribution of the ion beam relative to the width of the "slice" of ions accumulated during one pass through the cell. For example, the accumulation efficiency of an ideal mono-energetic ion beam would not be improved by doubling the accumulation bandwidth (say from 0.5 eV/q to 1.0 eV/q) as the entire ion ensemble would be sufficiently decelerated during the initial traversal of the trapped ion cell (provided that the accumulation potentials were set slightly below the kinetic energy of the impinging ion beam). Fig. 3 illustrates the effect of doubling the kinetic energy acceptance bandwidth for two ion beams with different kinetic energy distributions. The kinetic energy distribution of both ion beams is a Gaussian distribution centered at 10 eV/q. The narrower distribution in (a) has a standard deviation of 0.1, while the distribution in (b) has a standard deviation of 0.2; the full width half maximum peak widths for the distributions in (a) and (b) are 1.2 and 2.4 eV/q, respectively. In this example it is assumed that each traversal of the trapped ion cell results in the accumulation of a 0.8 eV/q "slice" of the ion population. If the trapping potentials are set to 8.8 V during ion accumulation, ions impinging on the trapped ion cell which have kinetic

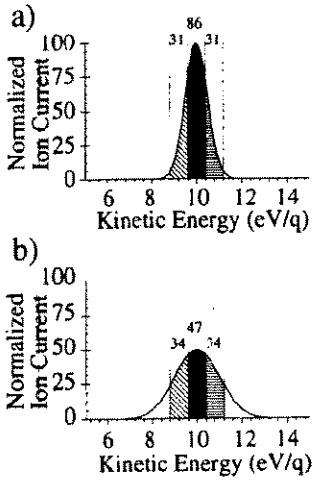

Fig. 3. Comparison of accumulation efficiency for two ion beams which have a Gaussian kinetic energy distribution centered around 10 eV/q with a standard deviation of (a) 0.1 and (b) 0.2. The enhancement in accumulation efficiency resulting from doubling the kinetic energy accumulation range is dependent on the width of the kinetic energy distribution relative to the accumulation bandwidth. The numbers above each section represent the normalized peak area of that section.

energies (E_k in eV/q in the range $8.8 < E_k < 9.6$ eV/q) will be trapped. Integration of the kinetic energy profiles between $E_k = 8.8$ eV/q and 9.6 eV/q yields a normalized ion abundance of collisionally accumulated ions. In this example the integrated peak areas from $8.8 < E_k < 9.6$ eV/q are 30.9 and 34.4 for (a) and (b) respectively. By doubling the accumulation bandwidths, the integrated peak areas from $8.8 < E_k < 10.4$ eV/q increase to 116.6 and 81.6, which translates into 3.8-fold and 2.4-fold enhancements in ion accumulation efficiency for (a) and (b) respectively. In this example, even if the initial accumulation potential is chosen to take a "slice" out of the middle of the ion distribution (i.e. $9.6 < E_k < 10.4$ eV/q), doubling the width of the "slice" results in a 40% or 70% improvement in ion accumulation for (a) or (b) respectively.

Fig. 2 compares the trapping efficiency using the three schemes in Fig. 1. The potentials on the x-axis represent those applied to (a) both trap plates and the auxiliary electrode, (b) the back trap plate and auxiliary electrode while the front plate is maintained at 5.5 V, and (c) the auxiliary electrode while both front and back trap plates are maintained at 5.5 V. In all cases, the trap plate potentials are dropped to 0.25 V prior to detection. Clearly, asymmetric accumulation potentials provide a significant enhancement in accumulation efficiency compared with the symmetric configuration. Fig. 2 also demonstrates that, when accumulating in an asymmetric well, ion intensity decreases with excessive asymmetry in the well because of the shallower trapping well. Accumulation with the auxiliary electrode scheme shows an increase in accumulation efficiency up to ≈ 15 V. Further experiments are underway to probe the effects of the position of the auxiliary electrode relative to the trapped ion cell. With the auxiliary electrode sufficiently displaced from the trapped ion cell, an external ion reservoir will form [30] which may result in additional enhancement in accumulation efficiency. The enhancement achieved using the auxiliary electrode compared with an asymmetric potential is apparent, as is the significant improvement realized when an asymmetric accumulation potential is utilized instead of a symmetric accumulation potential. Our experiments indicate that the three configurations utilized for accumulated trapping exhibit trapping efficiencies such that symmetric $\ll$ asymmetric $<$ auxiliary electrode.

3.4. Trapping potential during excite and detect

As described above, the relatively high pressure in the trapped ion cell during ion injection provides rapid z-axis cooling. The rapid relaxation of the trapping motion makes it feasible to decrease the trapping potential abruptly prior to excitation/detection, allowing transients to be acquired at a trapping voltage independent of the accumulation potential. This detection scheme affords two distinct advantages. First, as previously noted [26], lowering the trapping potentials often results in improved signal intensity, as transient lifetime is significantly increased when spectral acquisition takes place at reduced trapping potentials. If the trapping potential remains fixed throughout injection and detection, transient half lives are typically 30 ms or less. However, reducing the trapping potential to 500 mV during excitation and detection results in transient half lives in excess of 16 s and affords a significant enhancement in the signal-to-noise ratio. Additionally, even though the kinetic energy of the ion beam (and thus the optimum accumulation potential) may vary with time or be analyte dependent [27], utilization of the same trapping potential during detection obviates the need for multiple calibration files, as the observed cyclotron frequency is dependent

on the trapping potential applied during detection. Thus, from the standpoint of mass accuracy it is advantageous to use the same trapping potential consistently during detection.

4. Conclusions

The applications of FTICR to analytical problems, specifically those applications involving external ion generation, are rapidly expanding. FTICR is clearly at the forefront of high performance mass spectrometry; however, the requirement of ion trapping and the related difficulties associated with external source applications have been the major stumbling block preventing widespread, routine utilization of these techniques. Challenges which demand improved dynamic range and sensitivity are being met by an increased understanding of ion trapping mechanisms. The present work demonstrates several variations of the accumulated trapping technique, based on trapping voltage asymmetries, that will serve to increase the applicability and sensitivity of FTICR with any external ion source. Of particular importance is the preservation of the potential well profile during accumulation, made possible with the introduction of an auxiliary electrode. The additional electrode creates a maximum effective collisional path length for all ions entering the trapped ion cell, and results in a doubling of the kinetic energy range of ions which are amenable to collisional accumulation.

Acknowledgments

This research was supported by internal PNL exploratory research through the U.S. Department of Energy. Pacific Northwest Laboratory is operated by Battelle Memorial Institute for the U.S. Department of Energy through contract DE-AC06-76RLO 1830.

References

[1] A.G. Marshall and L. Schweikhard, Int. J. Mass Spectrom. Ion Processes, 118 (1992) 37.
[2] C. Koster, M.S. Kahr, J.A. Castoro and C.L. Wilkins, Mass Spectrom. Rev., 11 (1992) 495.
[3] A.G. Marshall and P.B. Grosshans, Anal. Chem., 63 (1991) A215.
[4] M.L. Gross, R.L. Cerny, D.E. Giblin, D.L. Rempel, D.K. Macmillan, P.F. Hu and C.L. Holliman, Anal. Chim. Acta, 250 (1991) 105.
[5] B. Asamoto, in Analytical Applications of Fourier Transform Ion Cyclotron Resonance Mass Spectrometry, VCH, New York, 1991, pp. 29.
[6] C.B. Lebrilla, I.J. Amster and R.T. McIver, Jr., Int. J. Mass Spectrom. Ion Processes, 87 (1989) R7.
[7] S.C. Beu, M.W. Senko, J.P. Quinn, F.M. Wampler and F.W. McLafferty, J. Am. Soc. Mass Spectrom., 4 (1993) 557.
[8] S.A. Hofstadler, E. Schmidt, Z. Guan and D.A. Laude, J. Am. Soc. Mass Spectrom., 4 (1993) 168.
[9] J.P. Speir, G.S. Gorman, C.C. Pitsenberger, C.A. Turner, P.P. Wang and I.J. Amster, Anal. Chem., 65 (1993) 1746.
[10] S.H. Guan, M.C. Wahl, T.D. Wood and A.G. Marshall, Anal. Chem., 65 (1993) 1753.
[11] L. Schweikhard, S.H. Guan and A.G. Marshall, Int. J. Mass Spectrom. Ion Processes, 120 (1992) 71.
[12] D.L. Rempel and M.L. Gross, J. Am. Soc. Mass Spectrom., 3 (1992) 590.
[13] J.E. Bruce, G.A. Anderson, S.A. Hofstadler, B.E. Winger and R.D. Smith, Rapid Commun. Mass Spectrom., 7 (1993) 700.
[14] S. Guan, M.C. Wahl and A.G. Marshall, Anal. Chem., 65 (1992) 3647.
[15] J.A. Castoro, C. Koster and C. Wilkins, Rapid Commun. Mass Spectrom., 6 (1992) 239.
[16] J.A. Carroll and C.B. Lebrilla, Org. Mass Spectrom., 27 (1992) 639.
[17] J.A. Carroll, L. Ngoka, C.G. Beggs and C.B. Lebrilla, Anal. Chem., 65 (1993) 1582.
[18] S.A. Hofstadler and D.A. Laude, Anal. Chem., 64 (1992) 569.
[19] B.E. Winger, S.A. Hofstadler, J.E. Bruce, H.R. Udseth and R.D. Smith, J. Am. Soc. Mass Spectrom., 4 (1993) 566.
[20] S.C. Beu, M.W. Senko, J.P. Quinn and F.W. McLafferty, J. Am. Soc. Mass Spectrom., 4 (1993) 190.
[21] P. Kofel and T.B. McMahon, Int. J. Mass Spectrom. Ion Processes, 98 (1990) 1.
[22] K.D. Henry, E.R. Williams, B.H. Wang, F.W. McLafferty, J. Shabanowitz, and D.F. Hunt, Proc. Natl. Acad. Sci. U.S.A., 86 (1989) 9075.
[23] S.A. Hofstadler and D.A. Laude, Jr., Int. J. Mass Spectrom. Ion Processes, 101 (1990) 65.

[24] S.C. Beu and D.A. Laude, Int. J. Mass Spectrom. Ion Processes, 104 (1991) 109.
[25] J.A. Castoro and C.L. Wilkins, Anal. Chem., 65 (1993) 2621.
[26] S.A. Hofstadler and D.A. Laude, J. Am. Soc. Mass Spectrom., 3 (1992) 615.
[27] S.A. Hofstadler and D.A. Laude, Anal. Chem., 65 (1993) 312.
[28] G. Scholes, Atomic and Molecular Beam Methods, Vol. 1, Oxford University Press, 1988, p. 15.
[29] D.A. Dahl and J.E. Delmore, SIMION, PC/PS2 version 4.0, Idaho National Engineering Laboratory (EGC-CS-7233, Rev. 2), April 1988.
[30] S.A. Hofstadler and D.A. Laude, Jr., Int. J. Mass Spectrom. Ion Processes, 97 (1990) 151.